
Baba Ismail YM, Ferreira AM, Bretcanu O, Dalgarno K, El Haj AJ.
[Polyelectrolyte multi-layers assembly of SiCHA nanopowders and collagen type I on aminolysed PLA films to enhance cell-material interactions.](#)

Colloids and Surfaces B: Biointerfaces 2017, 159, 445-453.

Copyright:

© 2017. This manuscript version is made available under the [CC-BY-NC-ND 4.0 license](#)

DOI link to article:

<https://doi.org/10.1016/j.colsurfb.2017.07.086>

Date deposited:

17/04/2018

Embargo release date:

14 August 2018



This work is licensed under a
[Creative Commons Attribution-NonCommercial-NoDerivatives 4.0 International licence](#)

**Polyelectrolyte multi-layers assembly of SiCHA nanopowders and collagen type I
on aminolysed PLA films to enhance cell-material interactions**

Yanny Marliana Baba Ismail^{1,2*}, Ana Marina Ferreira³, Oana Bretcanu³, Kenneth
Dalgarno³, Alicia El Haj²

¹School of Materials and Mineral Resources Engineering, Universiti Sains Malaysia,
Engineering Campus, 14300, Nibong Tebal, Penang, Malaysia.

²Guy Hilton Research Centre, Institute for Science and Technology in Medicine,
Keele University, Thornburrow Drive, Hartshill, Stoke-on-Trent, ST47QB, United
Kingdom.

³School of Mechanical and Systems Engineering, Newcastle University, Newcastle-
upon-Tyne, NE17RU, United Kingdom.

Corresponding author: Dr. Yanny Marliana Baba Ismail

Email: yannymarliana@usm.my

Tel: +604-5996154

Fax: +604-5996097

Abstract

This paper presents a new approach to assembling bone extracellular matrix components onto PLA films, and investigates the most favourable environment which can be created using the technique for cell-material interactions. Poly (lactic acid) (PLA) films were chemically modified by covalently binding the poly(ethylene imine) (PEI) as to prepare the substrate for immobilization of polyelectrolyte multilayers (PEMs) coating. Negatively charged polyelectrolyte consists of well-dispersed silicon-carbonated hydroxyapatite (SiCHA) nanopowders in hyaluronic acid (Hya) was deposited onto the modified PLA films followed by SiCHA in collagen type I as the positively charged polyelectrolyte. The outermost layer was finally cross-linked by 1-ethyl-3-(3-dimethylaminopropyl) carbodiimide hydrochloride and N-hydroxysulfosuccinimide sodium salt (EDC/NHS) solutions. The physicochemical features of the coated PLA films were monitored via X-ray Photoelectron Spectroscopy (XPS) and Atomic Force Microscope (AFM). The amounts of calcium and collagen deposited on the surface were qualitatively and quantitatively determined. The surface characterizations suggested that 5-BL has the optimum surface roughness and highest amounts of calcium and collagen depositions among tested films. *In vitro* human mesenchymal stem cells (hMSCs) cultured on the coated PLA films confirmed that the coating materials greatly improved cell attachment and survival compared to unmodified PLA films. The cell viability, cell proliferation and Alkaline Phosphatase (ALP) expression on 5-BL were found to be the most favourable of the tested films. Hence, this newly developed coating materials assembly could contribute to the improvement of the bioactivity of polymeric materials and structures aimed to bone tissue engineering applications.

Keywords: silicon-carbonated hydroxyapatite, collagen type I, hyaluronic acid, poly (lactic acid), polyelectrolyte multilayers coating, cell-material interaction, mesenchymal stem cells

1. Introduction

Scaffolds are three-dimensional (3D) biomaterials which guide cells growth and activities, the synthesis of biological molecules particularly the extracellular matrix (ECM), and to facilitate the formation of functional tissues and organs¹⁻³. From biological perspective, advanced biomaterials used in the fabrication of scaffolds must possess excellent biocompatibility, biodegradability as well as the ability to provide necessary physical and chemical cues to guide cell attachment, proliferation and differentiation^{4,5}. This will subsequently lead to the formation of 3D tissues. However, initially most biological reactions occur at the surfaces and interfaces^{6,7}. Among various biomaterials which have been investigated in the biomedical field, Poly (lactic acid), PLA is one of the synthetic polymers that has been widely used as a substrate material to support the regeneration of tissues and organs, including bone and articular cartilage^{7,8}. PLA is non-toxic, induces low levels of immunogenic reaction, has easily tailored mechanical properties as well as predictable degradation rates⁹. However, applications of PLA in the biomedical field have been hindered by its hydrophobicity and lack of cell recognition, poor cell adhesion and proliferation^{10,11}.

As tissue engineering (TE) scaffolds interact with the biological environment via their surface, modification on the outermost surface of the materials is considered as an effective approach^{12,13}. The main aim in surface modification of a polymer substrate is to provide a surface with reactive groups such as -OH, -NH₂ and -COOH to permit binding with biomolecules⁹. To further enhance the surface properties, surface modification could be followed by a layer-by-layer (LBL) coating also known as Polyelectrolyte Multilayer (PEM) assembly^{7,14}. LBL is a promising technique to modify surfaces in a controlled manner and has been employed in the fabrication of different reservoir/barrier architecture containing biomolecules, biosensors and nonlinear optical devices, due to its simplicity and versatility^{14,15}. This technique permits the construction of multilayer films simply by alternating deposition of oppositely charged polyions^{16,17}. An ideal bone scaffold, designed to enhance bone formation, should closely mimic the naturally occurring environment in the bone matrix, which is composed of hydroxyapatite (HA) crystals, collagen type I and proteoglycans. These biomacromolecules can then form physical or chemical cross-

linked networks, which regulate the expression of osteoblastic phenotype and supports osteogenesis *in vitro* and *in vivo*^{18,19}. Therefore, many natural ECM-like biomacromolecules have been integrated into 3D scaffolds for bone regeneration. To achieve this, LBL seems as an attractive fabrication technique as it allows defined deposition of biomolecular polyelectrolytes on the substrates, which mimic the natural formation of the biological world that is built-up via precise self-assembly^{19–21}.

Herein, we describe a newly develop ECM-like coating materials assembly onto the biodegradable PLA by aminolysis surface modification followed by PEMs assembly. The rationale behind the selection of silicon-carbonated HA (SiCHA), hyaluronic acid and collagen type I as the building blocks of the coating materials used was to generally replicate the natural bone ECM biomacromolecules (Fig. 1). SiCHA nanopowders were used as the major inorganic component to closely mimic bone mineral composition as bone typically consists of $\text{Ca}_{10}(\text{PO}_4)_6(\text{OH})_2$ with 2-8wt% carbonate and <1wt% Si^{22–24}. On the other hand, Hyaluronic acid (Hya) is a major component in ECM and synovial fluid. It is one of the polyanions which has been widely used in PEMs assembly^{20,25}. Collagen type I (Coll I) is also an important ECM component and is positively charged below the isoelectric point, which allows it to be used as a polycation⁷. In this study, the bilayers were finally cross-linked with 1-ethyl-3-(3-dimethylaminopropyl) carbodiimide hydrochloride and N-hydroxysulfosuccinimide sodium salt (EDC/NHS) so as to maximize the coating materials deposition. PLA films were coated with different deposition cycles to investigate the most favourable growth environment for cell-material interaction in order to fabricate ECM-based films or scaffolds for bone tissue engineering (BTE) applications.

2. Materials and Methods

2.1. Fabrication of PLA films

PLA resin (NatureWorks® LLC, United States) was dissolved in 1, 4 Dioxane (Sigma-Aldrich, United Kingdom) (30 mg/mL) at 70°C for three hours using a magnetic stirrer to obtain a homogenously dissolved solution. The viscous translucent solution was carefully cast into a glass petri dish, so as to prevent any bubble formation. The glass culture dish was then covered with parafilm, with small pores

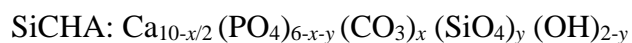
created on the top of the parafilm to permit slow evaporation of the solvent, and left in a fume cupboard overnight. This produced a PLA film of 5 μm thickness. The film was removed from the petri dish and cut into 1 mm squares.

2.2. Surface modification of PLA films

The surface of the PLA films was modified by introducing amino functional groups through aminolysis. The mechanisms involved in aminolysis on PLA films is demonstrated Fig. 2(a). The PLA films were immersed in 0.1 M sodium hydroxide, NaOH (Sigma-Aldrich, United Kingdom) for 20 minutes and then rinsed in distilled water for 5 minutes. The films were washed in 1:1 v/v of ethanol/water solution for 30 minutes and then washed in distilled water for 5 minutes. Afterwards, the PLA films were transferred into a mixture of EDC/NHS solution (3 and 5 mg/mL respectively, pH 6.0) under constant shaking (EDC; (ThermoFisher Scientific, United Kingdom, NHS; Sigma-Aldrich, United Kingdom). The films were then washed with distilled water. Finally, the films were immersed in 10 mg/mL poly (ethylene imine) solution (PEI; Sigma-Aldrich, United Kingdom) at pH 7.4 and stirred for 3 hours at 40°C followed by washing thoroughly in large amounts of distilled water for 15 minutes before being left to dry overnight.

2.3. Preparation of SiCHA nanopowders

The SiCHA nanopowders were synthesised by nanoemulsion method at room temperature using analytical grade $\text{Ca}(\text{NO}_3)_2 \cdot 4\text{H}_2\text{O}$, $(\text{NH}_4)_2\text{HPO}_4$, NH_4HCO_3 and $\text{Si}(\text{CH}_3\text{COO})_4$. All reagents were purchased from Sigma-Aldrich, United Kingdom. The amounts of carbonate, CO_3^{2-} (x) and silicate, SiO_4^{4-} (y) substituted into the apatite structure were calculated based from the following stoichiometry empirical formula;



where $x= 2.0$ and $y= 0.3$ moles. The synthesised nanopowders were then calcined at 500°C in air atmosphere with a heating rate of 10°C /min and at least one hour soaking time.

2.4. Build-up of the polyelectrolyte multi-layered films (PEMs)

The PEMs technique was developed from that previously described by Zhao et al.⁷ to include substituted hydroxyapatite nanopowders. The polyelectrolytes were first prepared:

- (i) 0.5 g of SiCHA nanopowders (average size = 100.12 ± 70.86 nm) were dispersed in hyaluronic acid solution (Lifecore Biomedical, United States) at concentration of 1.0 mg/mL and this served as the polyanion solution.
- (ii) the polycation solution was prepared by dispersing 1.0 g of the SiCHA nanopowders in 2.0 mg/mL collagen type I (high concentration rat tails; BD Bioscience, United Kingdom).
- (iii) A coupling agent consisted of 3 mg/mL EDC mixed with 5 mg/mL NHS solutions was used to cross-link the PEMs assembly.

All the solutions prepared were adjusted to pH 5.0. The modified PLA films were firstly immersed into the polyanion solution for 15 minutes followed by rinsing in ultrapure water (pH 5.0). After washing, the films were immersed into the polycation solution for 15 minutes. The films were then washed again in fresh ultrapure water (pH 5.0). EDC/NHS solution was then introduced at the final step at the outermost layer followed by washing in ultrapure water. 1, 3, 5 and 10 bilayer coatings were applied, by repeating the steps above (Fig. 2b). The coated films were then dried at room temperature overnight.

2.5. Physico- chemical Characterization

2.5.1. Analysis of Surface Composition

XPS is an exceptionally sensitive tool to investigate the chemical elements constituting the outermost layer of a surface approximately up to 200 Å. The films were analysed using K-Alpha^{TM+} XPS Instrument (Thermo Scientific, United States). The relative atomic concentrations were determined from the C1s, O1s, Ca2p, P2p, N1s, and Si2p at binding energy (BE) of 288.9, 533.0, 349.0, 135.0, 400.0, and 101.0, respectively using the built-in CasaXPS software. In order to detect the BE representing the chemical binding states of the each elements within the films, the XPS spectra for the chemical elements detected from the films were subjected to peak

deconvolution using a peak analysis program^{7,25-27}.

2.5.2. Analysis of Surface Topography

The surface topography of the PLA films before and after coating with different number of bilayers was observed using an atomic force microscope (AFM) in tapping mode using BioScope Catalyst AFM (Bruker, Germany) with ScanAsyst Adaptive Mode at ambient condition. The PLA films were imaged using an RTESPA tip of spring constant 4 N/m, 896 scans/lines, 0.32 Hz scan rates, and 1.102 V amplitude²⁸. The scan area was a 1 mm square. At least 3 samples were imaged to calculate the surface roughness for both whole and localised areas of the films. The term “whole area” refers to the entire scan area of 1 mm²; “localised area”, means spot areas of 1 nm² within the “whole area”.

2.5.3. Quantification of calcium and collagen distributions

Calcium is chelated by alizarin red S (ARS) in aqueous solution, forming a complex which can subsequently dissociate. A 1 w/v% solution of ARS in dH₂O was prepared and adjusted to pH 10.0 using ammonium hydroxide. 1 mL of ARS aqueous solution was added on the surface of the 1 mm square PLA films placed in a 24 well culture plate and allowed to incubate for 10 minutes. The unbound calcium stain was carefully removed in several changes of dH₂O followed by drying and immediately imaged using a bright field microscope AMG-EVOS X1 CORE with a magnification of 4X. To further quantify the calcium deposition, 1 mL of 2 w/v% cetylpyridinium chloride monohydrate was then added directly to the relevant wells. The absorbance of the resulting solution was measured at 562 nm.

The qualitative distribution of collagen type I (Coll I) on multi-layered PLA films were examined by staining using Sirius Red (SR) solutions. Samples ($n=3$) were imaged using a bright field microscope AMG-EVOS x1 CORE with a magnification of 4X. The colorimetric ninhydrin method was used to further quantify the multi-layered Coll I content. The PLA film was placed in 1 mL of 6 M HCl and 4 mL of Phosphate Buffered Saline (PBS) solution and heated at 120°C under a nitrogen atmosphere for 6 hours to hydrolyze the collagen to amino acids. After the centrifugation of the resultant solution, 1 mL of the supernatant was neutralized with 1 M NaOH followed by the addition of ninhydrin reagent solution (Sigma-Aldrich,

United Kingdom). The solution was boiled for 15 min to ensure complete colour development and then cooled to room temperature. After adding 5 ml of 50% ethanol, the absorbance at 570 nm was measured by using a UV spectrophotometer (UV-1601, Shimadzu). Collagen content was determined using a standard calibration curve from known amounts of collagen while subtracting the contribution from the aminolysed PLA film.

2.6. hMSCs culture and seeding on multi-layered PLA films

Human bone marrow derived-mesenchymal stem cells (hMSCs) obtained from a 24-year old male (Lonza, United States) were initially characterized upon isolation by evaluating their multi-lineage differentiation and the expression of key cell CD bone surface markers (CD73, CD90, CD105, CD14, CD19, CD34 and HLA-DR) which were quantified qualitatively using immunostaining and quantitatively by flow cytometry (data for hMSCs characterization are not shown in this paper). The same batch of cells was used for the characterization of hMSCs were expanded in 75 cm² tissue culture flasks in a humidified environment at 37°C with 5% CO₂ until passage two at 80% confluent. Cells were cultured in basal media containing 1% L-glutamine (Lonza, United Kingdom), 1% Penicilin Streptomysin (Lonza, United Kingdom) and 10% Fetal Bovine Serum (Biosera labtech, United Kingdom) in 4.5 g/L Dulbecco's Modified Eagle Medium (Lonza, United Kingdom). Prior to cell seeding, the multi-layered PLA films were sterilized in UV chamber for three cycles for 90 seconds/cycle. 50,000 cells (200 µL cell suspension/film) at passage three were directly seeded on the surface of the 1 mm² PLA films placed in a 24-well culture plate and were incubated for 3 hours in a humidified atmosphere to allow cell attachment. Afterwards, culture medium was added to a final volume of 1.5 mL and the cell/multi-layered PLA films were incubated for 14 days. The media was changed every three days.

For each time-point, cells/multi-layered PLA films were rinsed with PBS, trypsinized, washed again with PBS and finally lysed in 1 mL of dH₂O followed by being frozen at -80°C. After three cycles of freeze/thaw, the samples were ready for the cytotoxicity assessment.

2.7. Cell viability

Cell viability was observed using a Confocal Laser Scanning Microscope (CLSM; Olympus Fluoview FV 1200 with Fluoview Version 4.1 software; Olympus, UK). The viability of the cells was assessed at 7 and 14 days using the Live/Dead Assay Kit (Invitrogen, United Kingdom) according to the manufacturer's instructions. Calcein-AM ester was used to fluorescently label viable cells (green); the nucleus of dead cells is labelled with Propidium Iodide (red). Briefly, cell culture media was removed from the relevant wells. The samples were washed with PBS then immersed in a PBS staining solution containing 10 μM Calcein-AM and 1 μM Propidium Iodide and incubated at 37°C for 20 minutes in the dark. The samples were then washed once with 1 mL of PBS and immediately imaged using CLSM.

2.8. Cell proliferation

The Quant-iT™ Picogreen® dsDNA assay kit (Invitrogen, United Kingdom) was used to indicate proliferation of hMSCs. The Picogreen solution was prepared as 1:200 dilutions in 1XTris-EDTA (TE) buffer (TE stock diluted in dH₂O) according to the manufacturer's instruction. Ranges of DNA dilutions (0-2 $\mu\text{g}/\text{mL}$ of DNA stock in 1XTE buffer) were used to construct a standard curve. 100 μL of cell lysate or DNA standard was placed in each well of a 96-well culture plate, followed by adding 100 μL of Picogreen reagent to each well. The plate was placed in the dark for 5 minutes before reading the fluorescence at 485/535 nm (excitation/emission) using a Synergy II BioTek plate reader.

2.9. Osteogenic differentiation

Alkaline phosphatase (ALP) activity was used to infer early osteogenic differentiation. Ranges of 4-Methylumbelliferone (4-MU; Sigma-Aldrich, Switzerland) dilutions (0-2 $\mu\text{g}/\text{mL}$ of 4-MU in dH₂O) were used to construct a standard curve. 50 μL of the cell lysate from each sample or standard of 4-MU and 50 μL of 4-MUP (4-MUP; Sigma-Aldrich, United Kingdom) were then added into the relevant well of 96-well culture plate, followed by incubation at 37°C for 90 minutes.

To terminate the reaction, 100 μ L of 1XTE was added and the fluorescence reading of the fluorescence was taken at 360/440 nm (excitation/emission).

2.10 Statistical analysis

Quantitative data were presented as means \pm standard deviation (SD). Data were initially tested for normality using the Kolmogorov-Smirnov test, with Dallal-Wilkinson-Lillie for corrected P value. A two-way ANOVA with multiple comparisons Tukey test were performed to optimize the number of multilayer depositions on the PLA films. Statistical significance was considered for $p \leq 0.05$ (*), $p \leq 0.01$ (**), $p \leq 0.001$ (***) and $p \leq 0.0001$ (****). All statistical analyses were performed using GraphPad Prism 7 software. For bioassays, tests were performed on $n=3$ in duplicates.

3. Results

3.1. Surface characterization

For unmodified PLA (0-BL), only two main peaks appeared in the XPS spectra (Fig. 3a), representing the elements of carbon (C1s) and oxygen (O1s), which were detected at binding energies of 288.9 and 533.0 eV. After surface modification (0-BL*), an additional elemental peak for nitrogen (N1s) was detected at 400.0 eV (Fig. 3b). After coating (Fig. 2b), a new calcium peak emerged (Fig. 3c-f). The typical peak of P2p and Si2p at binding energies of 135.0 and 101.0 eV, were not clearly evident on the XPS scan spectra but detected by using the CasaXPS software. With increasing number of bilayers coating on the substrates, the intensity of the nitrogen (N1s) peak proportionally increased till it reached a maximum at 5-BL.

The atomic percentage of the control PLA (0-BL) and coated PLA with 1-, 3-, 5- and 10-BL obtained from the XPS survey spectra are shown in Table 1. The carbon content of the PLA film reduced from 77.7 at% (0-BL) to 74.6 at% (0-BL*). However, no significant differences were detected in the C1s and O1s contents of the coated films relative to the modified PLA films (0-BL*) ($p \geq 0.05$). It was observed that the level of N1s increases from 0-BL to 5-BL deposition cycles. When compared between the coated films, the level of N1s on 5-BL was significantly higher than 3-BL ($p \leq 0.01$) and 10-BL ($p \leq 0.001$). Concurrently, higher Ca2p and P2p atomic

percentages were observed with increasing numbers of layers up to 5-BL ($p \leq 0.0001$). The percentages of Ca₂ and P_{2p} detected on 10-BL were significantly decreased compared to 5-BL ($p \leq 0.01$). Si_{2p} peak was also found on all multi-layered PLA films. The highest atomic percentages of Ca_{2p}, P_{2p}, Si_{2p} and N_{1s} (which represent the chemical composition of the coating materials) were obtained on 5-BL PLA films.

The surface roughness of the control and coated PLA films measured by AFM showed no significant differences between the roughness of the whole film and individual, localized areas on each film ($p \geq 0.05$) as shown in Table 2. The surface roughness increased with increasing number of layers up to 5-BL ($p \leq 0.0001$). The surface roughness of 1-BL PLA films was approximately twice as rough as the unmodified control PLA films ($p \leq 0.0001$). However, only a slight increase in surface roughness was observed after the third alternate deposition of the coating materials ($p \leq 0.01$). Further deposition (>5-BL) resulted in a small drop in surface roughness ($p \leq 0.05$).

Positive Alizarin Red (AR) staining (bright red, with brightness proportional to calcium content) was obtained from all the coated PLA films as demonstrated in Fig. 4a. More homogenous bright red staining was observed on the PLA film surface with increased deposition cycles as can be seen on 3-, 5- and 10-BL relative to 1-BL coated films. The bright orange stain of Sirius Red (SR) indicated a positive result for the presence of collagen. The brightness of the stain is directly proportional to the amount of collagen present within the multi-layered films. The control PLA films (0-BL) showed an absence of both AR and SR staining. Quantitatively, the amount of deposited calcium and collagen on the multi-layered PLA films grew linearly up to 5-BL and levelled out or dropped slightly (Fig. 4b). The trends obtained were well correlated with the aforementioned surface compositions and surface roughness analyses.

3.2. In vitro biocompatibility assessments

The viability of hMSCs seeded on different deposition cycles of the multi-layered PLA films was observed after 7 and 14 days of culture (Fig. 5). CLSM images demonstrated that cells were homogeneously distributed on the surface of all coated

PLA films. However, the cell density appeared to be less confluent on unmodified, control PLA films (0-BL), relative to their coated counterparts.

The extent of cell proliferation was estimated by DNA quantification (Fig. 6a). Overall, the deposition of the innovative coating materials assembly on the PLA films resulted in increased cell proliferation over the culture period ($p \leq 0.0001$) and differed between the coated films ($p \leq 0.0001$). There was a significant interaction between time and coated film ($p \leq 0.05$) suggesting that the increase in DNA concentration over time differed between coated films. Overall, the highest DNA contents were obtained by culturing hMSCs in direct contact with 5-BL coated films compared to all tested films (non-coated and coated films) on day 7 and day 14 ($p \leq 0.0001$).

The early osteogenic differentiation of the hMSCs cultured on the control (unmodified) and coated PLA films was assessed by measuring their ALP activity after culturing for 7 and 14 days in basal media. The ALP activity shown in Fig. 6b represented the values of ALP normalised to DNA concentration. Regardless of the number of deposition cycles on the PLA films, significantly higher levels of mean ALP activity were obtained when hMSCs were cultured on the coated films than the control on day 7 and day 14 ($p \leq 0.0001$). hMSCs cultured on 5-BL coated films exhibited the highest levels of mean ALP activity on day 7 and 14 ($p \leq 0.0001$) as compared to all other tested films.

4. Discussion

Surface properties of a biomaterial such as topography, chemical composition and hydrophilicity can regulate cell-material interactions^{8,29,30}. These properties greatly influence the viability and functional activity of anchorage-dependent cells such as hMSCs and osteoblasts. In this study, the surface properties of the hydrophobic PLA films were improved, which subsequently enhanced cell biocompatibility in direct contact with the substrates. The extracellular matrix components HA-based materials and collagen type I have been successfully deposited onto the aminolysed PLA films using PEMs technique.

XPS analysis confirmed that PLA films were effectively modified by aminolysis process, as identified by the presence of N1s peak. Increasing number of layers means

more collagen deposited on the surface, which is associated with the increase of amino acid residues on the surface³¹. As a consequence, the intensity of N1s peak appeared higher on the coated PLA films with increasing deposition cycles compared to the aminolysed PLA films. The introduction of amino functional groups through aminolysis provides a positive charge on the surface, which allows the alternate absorption of polyanion (SiCHA in hyaluronan) followed by polycation (SiCHA in Collagen type I) solutions. The introduction of the coating materials assembly induces a rougher surface area and provides recognition sites (i.e. from collagen) for better cell attachment on the films compared to the unmodified PLA films. 5-BL coated films possessed the highest surface roughness of all the groups tested. However, after 5 deposition cycles, there was a small drop in the surface roughness of the 10-BL coated films. This result was consistent with the findings reported in the literature¹⁴. Subsequent deposition of polyelectrolytes serves to fill voids and defects present in previous layers of the coating, effectively creating a smoother surface³². It is also believed that after finite *n*-layers deposition (which varies depending on the materials used), the electrostatic force binding the polyelectrolytes become weaker and the surface might have reached the saturated level of absorption³³. This can be explained from the surface characterization analyses, where the saturation level of absorptions has been reached after 5-BL deposition cycles. Thus, increasing number of coating layers up to 10-BL could cause collapse of the layers formed as the coating materials fail to properly bind to the surface.

Besides surface roughness, the chemical composition also plays an important role in cell responses. The presence of the bilayer coating played an important role in favouring the cellular adhesion and proliferation on the surface predominantly on poor cell recognizable and hydrophobic substrates such as PLA³⁴⁻³⁶. Currently, much effort is being devoted to engineer the surfaces of biomaterials to achieve the required biologic responses since substrate physiochemical features have a significance impact on the protein absorption and its functional activity, subsequently determining cell fate³⁷. Among the most investigated coating materials to improve the surface properties of PLA substrate are poly(styrene sulfonate sodium salt), chitosan, hyaluronic acid and collagen type I^{7,14,35,38}. In this investigation, we were able to develop new coating materials consisting of silicon-carbonated doped hydroxyapatite (SiCHA) nanopowders dispersed in hyaluronic acid and collagen type I. This newly

developed coating materials assembly showed no toxicity effects after 14 days with more viable cells were found on the coated PLA films than the control PLA films (unmodified). A similar observation was reported in literature where upon culturing MG63 osteoblast-like cells on collagen-nano HA scaffolds and collagen scaffolds. These results confirmed that the coating materials invented are biocompatible and lead to better cell viability³⁹.

Among the bilayer components, collagen is known to contain an adhesion sequence (RGD), which favours cell attachment and proliferation⁴⁰⁻⁴³. Regardless of the deposition cycles, all coated PLA films encouraged more rapid cell proliferation. Consistent with the hMSCs viability and proliferation, the coated PLA films exhibited an encouraging improvement in osteogenic activity relative to the unmodified films. This indicated that the coating materials assembly is not only biocompatible but both osteoconductive and osteoinductive as they provide a suitable basis that could accelerate matrix-mediated intracellular signalling related to osteoblastic activity²⁷. Moreover, this result demonstrated the efficacy of the SiCHA nanopowders on the surface, which not only improved cell adhesion by providing rougher surface but also enriched the osteoblastic phenotype expression level. This explained our observation that the highest cell proliferation level and ALP activity was obtained on the coated PLA films and in particular 5-BL, which have the roughest surface and greatest presentation of the coating materials as compared to the other tested films. Several studies have demonstrated that calcium ions (a major component of HA) are directly involved in boosting the proliferation and osteoblast cell type phenotype expression through membrane-mediated ion transfer, which is a possible explanation for the results observe in this study^{39,44,45}. This highlighted the benefits of having both collagen type I and HA-based materials as major components in fabricating a hybrid scaffold with the aim to enhance bone formation.

From the results presented here, we can confirmed that the novel coating materials assembly established in this work is an effective approach to mimic native bone ECM in order to facilitate cell-material interactions and enhance cell functions such as cell viability, proliferation and differentiation of hMSCs, leading to a beneficial advancement for bone tissue engineering applications. Minimum manufacturing consumption with maximum performances is always the goal in large-scale

manufacture. We can summarize here that 5-BL fulfills this requirement, as increasing the number of deposition layers beyond 5 gave no improvement on the performance of the coating material.

5. Conclusions

The development of a bone ECM-like multi-layered assembly with silicon-carbonated HA (SiCHA) nanopowders, hyaluronic acid, collagen type I deposited by PEMs technique on aminolysed PLA films has effectively improved the cell-material interactions and bioactivity as compared to unmodified PLA films. The combination of osteoconductive (SiCHA nanopowders) and osteoinductive (collagen type I) materials as polyelectrolytes component up to 5-BL depositions resulted in the most favourable milieu for the hMSCs survival and functions, demonstrating a great potential for bone tissue engineering applications.

Acknowledgements

The authors would like to thank the Arthritis Research UK Tissue Engineering Centre (Award 19429) and the Ministry of Higher Education Malaysia (MOHE; Grant no.: R5240-B273) for supporting this work. We would like to thank the National EPSRC XPS Users Service (NEXUS), Newcastle University for conducting the XPS analysis and Dr. Clare Hoskins from Keele University for performing the AFM analysis

References

1. Hutmacher, D. W., Scaffolds in tissue engineering bone and cartilage. *Biomaterials* **21**, 2529–2543 (2000).
2. Song, K., Liu, T., Cui, Z., Li, X. & Ma, X., Three-dimensional fabrication of engineered bone with human bio-derived bone scaffolds in a rotating wall vessel bioreactor. *J. Biomed. Mater. Res. A* **86**, 323–32 (2008).
3. Dhandayuthapani, B., Yoshida, Y., Maekawa, T. & Kumar, D. S., Polymeric Scaffolds in Tissue Engineering Application: A Review. *Int. J. Polym. Sci.* **2011**, 1–19 (2011).

4. Parenteau-Bareil, R., Gauvin, R. & Berthod, F., Collagen-based biomaterials for tissue engineering applications. *Materials (Basel)*. **3**, 1863–1887 (2010).
5. Velasco, M. A, Narváez-Tovar, C.A & Garzón-Alvarado, D.A., Design, Materials, and Mechanobiology of Biodegradable Scaffolds for Bone Tissue Engineering. *Biomed Res Int*. **2015**, (2015).
6. Dimitriou, R., Jones, E., McGonagle, D. & Giannoudis, P. V., Bone regeneration: current concepts and future directions. *BMC Med*. **9**, 66 (2011).
7. Zhao, M.Y., Li, L.H., Zhou, C. R. LBL coating of type I collagen and hyaluronic acid on aminolyzed PLLA to enhance the cell-material interaction. *Express Polym. Lett*. **8**, 322–335 (2014).
8. Chen, Y, Mak, A.F.T., Wang, M., Li, J.S., Wong, M.S., In vitro behavior of osteoblast-like cells on PLLA films with a biomimetic apatite or apatite/collagen composite coating. *J. Mater. Sci. Mater. Med*. **19**, 2261–2268 (2008).
9. Suh, H., Hwang, Y. S., Lee, J. E., Han, C. D. & Park, J. C., Behavior of osteoblasts on a type I atelocollagen grafted ozone oxidized poly L-lactic acid membrane. *Biomaterials* **22**, 219–230 (2001).
10. Kim, S-S., Park, M.S., Jeon, O., Choi, C.Y., Kim, B. S., Poly(lactide-co-glycolide)/hydroxyapatite composite scaffolds for bone tissue engineering. *Scanning* **27**, 1399–1409 (2006).
11. JVanusca Dalosto Jahno, Gabriela Bendero ´vicz Mendes Ribeiro, Lui ´s Alberto dos Santos, Rosane Ligabue, Sandra Einloft, M. R. W. F. & Bombonato-Prado, K. F., Chemical synthesis and in vitro biocompatibility tests

- of poly (L-lactic acid). *J. Biomed. Mater. Res. A* **81**, 771–780 (2007).
12. Domke, J., Dannöhl, S., Parak, W.J. Müller, O., Aicher, W.K., Radmacher, M., Substrate dependent differences in morphology and elasticity of living osteoblasts investigated by atomic force microscopy. *Colloids Surfaces B Biointerfaces* **19**, 367–379 (2000).
 13. Tzoneva, R., Seifert, B., Albrecht, W., Richau, K., Groth, T., Lendlein, A., Hemocompatibility of poly(ether imide) membranes functionalized with carboxylic groups. *J. Mater. Sci. Mater. Med.* **19**, 3203–3210 (2008).
 14. Zhu, Y., Gao, C., He, T., Liu, X. & Shen, J., Layer-by-Layer Assembly To Modify Poly (L -lactic acid) Surface toward Improving Its Cytocompatibility to Human Endothelial. 446–452 (2003).
 15. Naves, A. F., Motay, M., Mérindol, R., Davi, C.P., Felix, O., Catalani, L.H., Decher, G., Layer-by-Layer assembled growth factor reservoirs for steering the response of 3T3-cells. *Colloids Surfaces B Biointerfaces* **139**, 79–86 (2016).
 16. Detzel, C. J., Larkin, A. L. & Rajagopalan, P., Polyelectrolyte multilayers in tissue engineering. *Tissue Eng. Part B. Rev.* **17**, 101–113 (2011).
 17. Hammond, P. T., Engineering materials layer-by-layer: Challenges and opportunities in multilayer assembly. *AIChE J.* **57**, 3199–3209 (2011).
 18. Datta, N., Holtorf, H. L., Sikavitsas, V. I., Jansen, J. A. & Mikos, A. G., Effect of bone extracellular matrix synthesized in vitro on the osteoblastic differentiation of marrow stromal cells. *Biomaterials* **26**, 971–977 (2005).
 19. Yu, H.-S., Jin, G.-Z., Won, J.-E., Wall, I. & Kim, H.-W., Macrochanneled

- bioactive ceramic scaffolds in combination with collagen hydrogel: a new tool for bone tissue engineering. *J. Biomed. Mater. Res. A* **100**, 2431–40 (2012).
20. Zhang, J., Senger, B., Vautier, D., Picart, C., Schaaf, P., Voegel, J.-C., Lavallo, P., Natural polyelectrolyte films based on layer-by layer deposition of collagen and hyaluronic acid. *Biomaterials* **26**, 3353–3361 (2005).
 21. Hoyer, B., Bernhardt, A., Heinemann, S., Stachel, I., Meyer, M., Gelinsky, M., Biomimetically mineralized salmon collagen scaffolds for application in bone tissue engineering. *Biomacromolecules* **13**, 1059–1066 (2012).
 22. Sprio, S., Tampieri, A., Landi, E., Sandri, M., Martorana, S., Celotti, G., Logroscino, G., Physico-chemical properties and solubility behaviour of multi-substituted hydroxyapatite powders containing silicon. *Mater. Sci. Eng. C* **28**, 179–187 (2008).
 23. Landi, E., Uggeri, J., Sprio, S., Tampieri, A. & Guizzardi, S., Human osteoblast behavior on as-synthesized SiO(4) and B-CO(3) co-substituted apatite. *J. Biomed. Mater. Res. A* **94**, 59–70 (2010).
 24. Shepherd, J. H., Shepherd, D. V & Best, S. M., Substituted hydroxyapatites for bone repair. *J. Mater. Sci. Mater. Med.* **23**, 2335–47 (2012).
 25. Botelho, C. M., Lopes, M. a, Gibson, I. R., Best, S. M. & Santos, J. D., Structural analysis of Si-substituted hydroxyapatite: zeta potential and X-ray photoelectron spectroscopy. *J. Mater. Sci. Mater. Med.* **13**, 1123–7 (2002).
 26. Shin, H.-Y., Jung, J.-Y., Kim, S.-W. & Lee, W.-K., XPS Analysis on Chemical Properties of Calcium Phosphate Thin Films and Osteoblastic HOS Cell Responses. *J. Ind. Eng. Chem.* **12**, 476–483 (2006).

27. Kim, T. G., Park, S.-H., Chung, H. J., Yang, D.-Y. & Park, T. G., Microstructured scaffold coated with hydroxyapatite/collagen nanocomposite multilayer for enhanced osteogenic induction of human mesenchymal stem cells. *J. Mater. Chem.* **20**, 8927 (2010).
28. Hoskins, C., Cuschieri, A. & Wang, L., The cytotoxicity of polycationic iron oxide nanoparticles: Common endpoint assays and alternative approaches for improved understanding of cellular response mechanism. *J. Nanobiotechnology* **10**, 15 (2012).
29. Wang, X., Zhou, Y., Xia, L., Zhao, C., Chen, L., Yi, D., Chang, J., Huang, L., Zheng, X., Zhu, H., Xie, Y., Xu, Y., Lin, K., Fabrication of nano-structured calcium silicate coatings with enhanced stability, bioactivity and osteogenic and angiogenic activity. *Colloids Surfaces B Biointerfaces* **126**, 358–366 (2015).
30. Surmeneva, M. A., Kleinhans, C., Vacun, G., Kluger, P.J., Schönhaar, V., Müller, M., Hein, S.B., Wittmar, A., Ulbricht, M., Prymak, O., Oehr, C., Surmenev, R.A., Nano-hydroxyapatite-coated metal-ceramic composite of iron-tricalcium phosphate: Improving the surface wettability, adhesion and proliferation of mesenchymal stem cells in vitro. *Colloids Surfaces B Biointerfaces* **135**, 386–393 (2015).
31. Zhang, Y., Wang, W., Feng, Q., Cui, F. & Xu, Y. A., Novel method to immobilize collagen on polypropylene film as substrate for hepatocyte culture. *Mater. Sci. Eng. C* **26**, 657–663 (2006).
32. Lowman, G. M. & Buratto, S. K., Nanoscale morphology of polyelectrolyte

- self-assembled films probed by scanning force and near-field scanning optical microscopy. *Thin Solid Films* **405**, 135–140 (2002).
33. Szilagyi, I., Trefalt, G., Tiraferri, A., Maroni, P. & Borkovec, M., Polyelectrolyte adsorption, interparticle forces, and colloidal aggregation. *Soft Matter* **10**, 2479–502 (2014).
 34. Kim, K., Yeatts, A., Dean, D., Fisher, J.P., Stereolithographic Bone Scaffold Design Parameters: Osteogenic Differentiation and Signal Expression. **16**, (2010).
 35. Liu, Z-M., Lee, S-Y., Sarun, S., Moeller, S., Schnabelrauch, M., Groth, T., Biocompatibility of poly(L-lactide) films modified with poly(ethylene imine) and polyelectrolyte multilayers. *J. Biomater. Sci. Polym. Ed.* **21**, 893–912 (2010).
 36. Guo, C., Guo, X., Cai, N. & Dong, Y., Novel fabrication method of porous poly(lactic acid) scaffold with hydroxyapatite coating. *Mater. Lett.* **74**, 197–199 (2012).
 37. Ribeiro, N., Sousa, S. R. & Monteiro, F. J., Influence of crystallite size of nanophased hydroxyapatite on fibronectin and osteonectin adsorption and on MC3T3-E1 osteoblast adhesion and morphology. *J. Colloid Interface Sci.* **351**, 398–406 (2010).
 38. Ferreira, A. M., Gentile, P., Toumpaniari, S., Ciardelli, G. & Birch, M. A., Impact of Collagen/Heparin Multilayers for Regulating Bone Cellular Functions. *ACS Appl. Mater. Interfaces* **8**, 29923–29932 (2016).
 39. Rodrigues, S.C., Salgado, C.L., Sahu, A., Garcia, M.P., Fernandes, A.H.,

- Monteiro, F.J., Preparation and characterization of collagen-nanohydroxyapatite biocomposite scaffolds by cryogelation method for bone tissue engineering applications. *J. Biomed. Mater. Res. - Part A* **101 A**, 1080–1094 (2013).
40. Bisson, I., Kosinski, M., Ruault, S., Gupta, B., Hilborn, J., Wurm, F. Frey, P., Acrylic acid grafting and collagen immobilization on poly(ethylene terephthalate) surfaces for adherence and growth of human bladder smooth muscle cells. *Biomaterials* **23**, 3149–3158 (2002).
41. Becker, D., Geibler, U., Hempel, U., Bierbaum, S., Scharnweber, D., Worch, H., Wenzel, K.W., Proliferation and differentiation of rat calvarial osteoblasts on type I collagen-coated titanium alloy. *J. Biomed. Mater. Res.* **59**, 516–527 (2002).
42. Ma, Z., Gao, C., Gong, Y. & Shen, J., Cartilage tissue engineering PLLA scaffold with surface immobilized collagen and basic fibroblast growth factor. *Biomaterials* **26**, 1253–1259 (2005).
43. Ferreira, A. M., Gentile, P., Chiono, V. & Ciardelli, G., Collagen for bone tissue regeneration. *Acta Biomater.* **8**, 3191–3200 (2012).
44. Liao, S. S., Cui, F. Z., Zhang, W. & Feng, Q. L., Hierarchically biomimetic bone scaffold materials: nano-HA/collagen/PLA composite. *J. Biomed. Mater. Res. B. Appl. Biomater.* **69**, 158–165 (2004).
45. Wahl, D. A. & Czernuszka, J. T., Collagen-hydroxyapatite composites for hard tissue repair. *European Cells and Materials* **11**, 43–56 (2006).

Figure 1

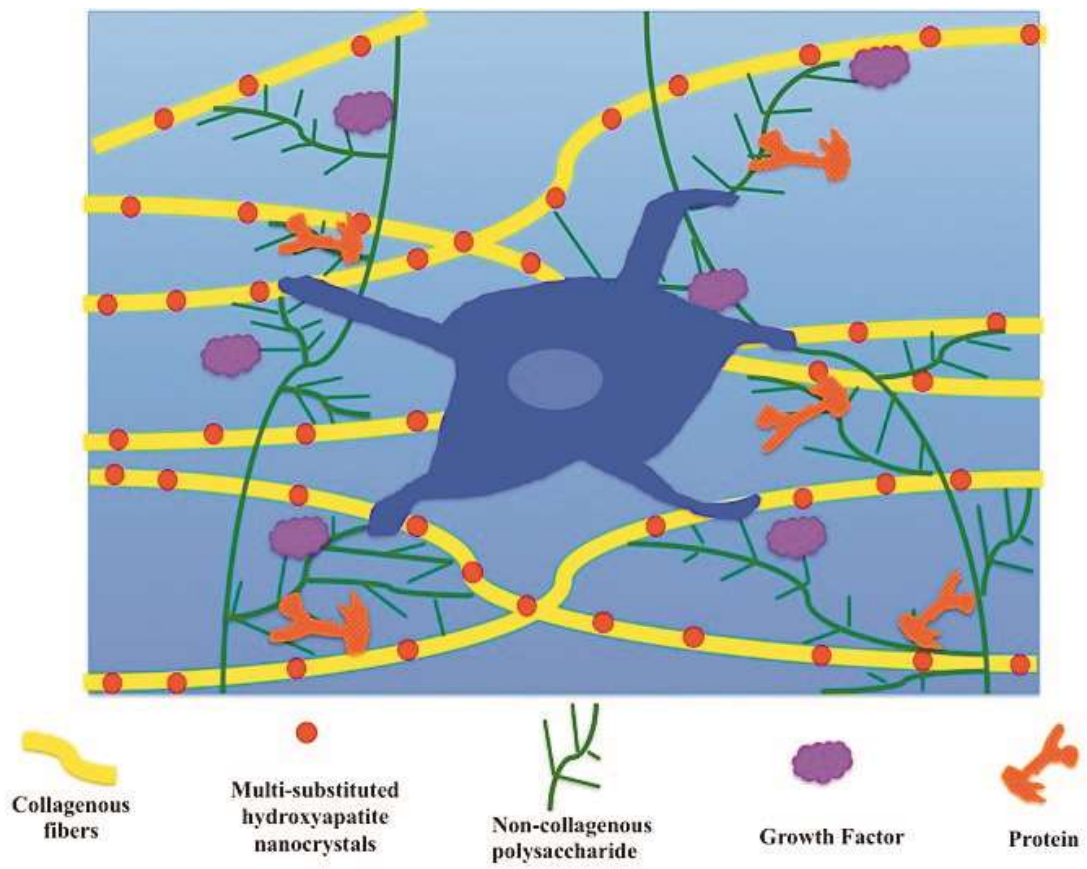
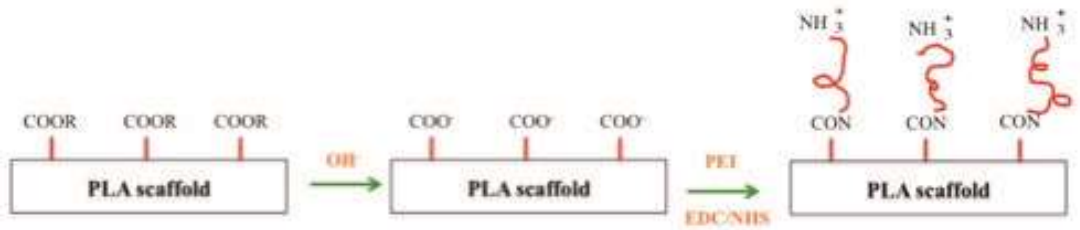
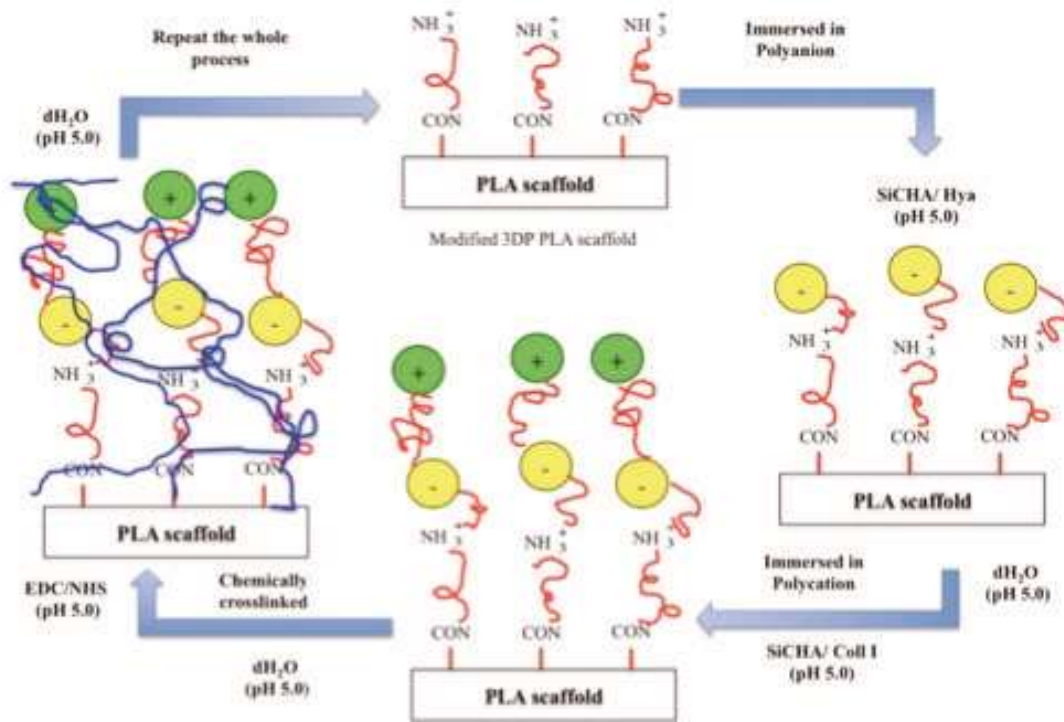


Figure 2



(a)



(b)

Figure 3

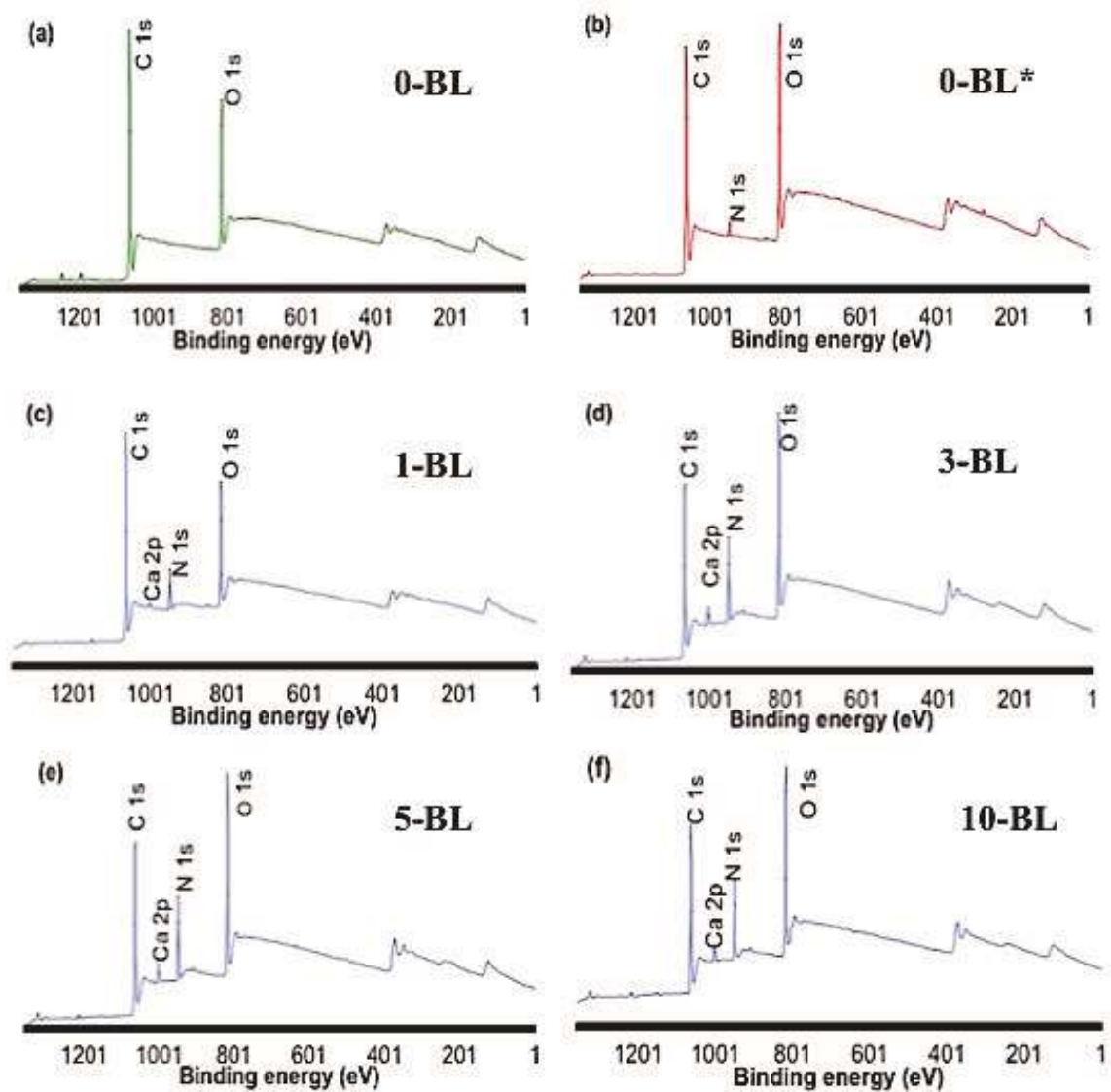


Figure 4

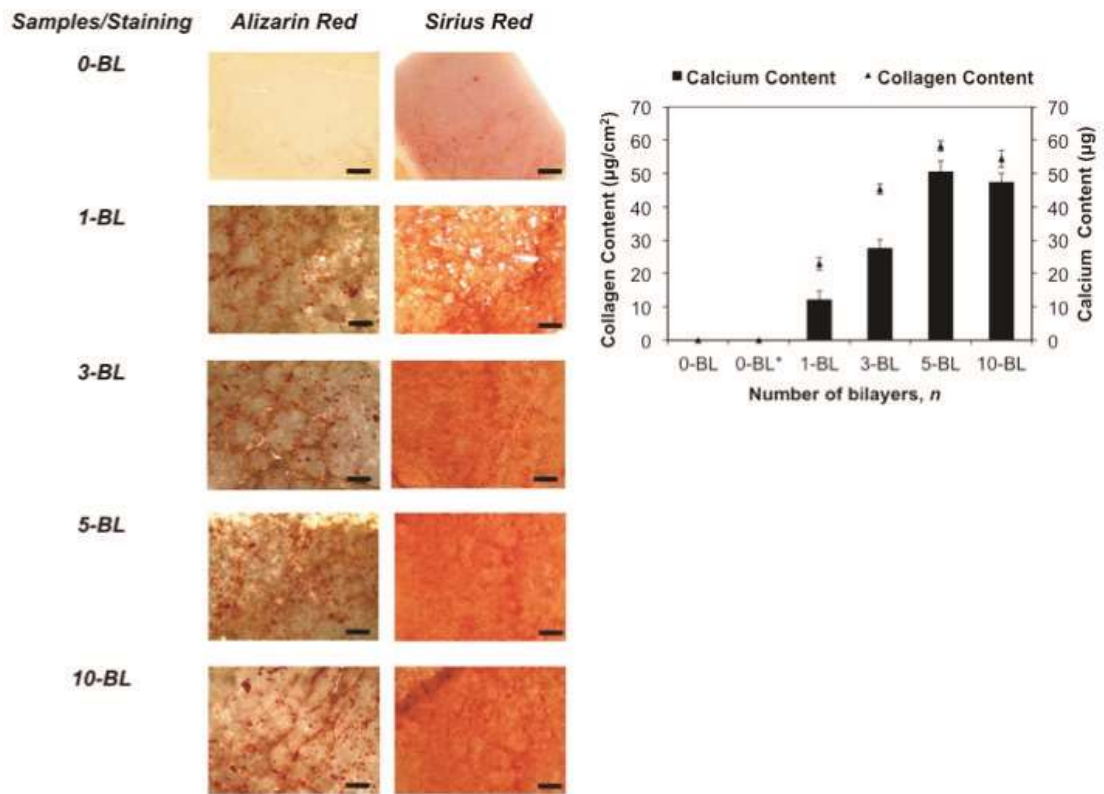


Figure 5

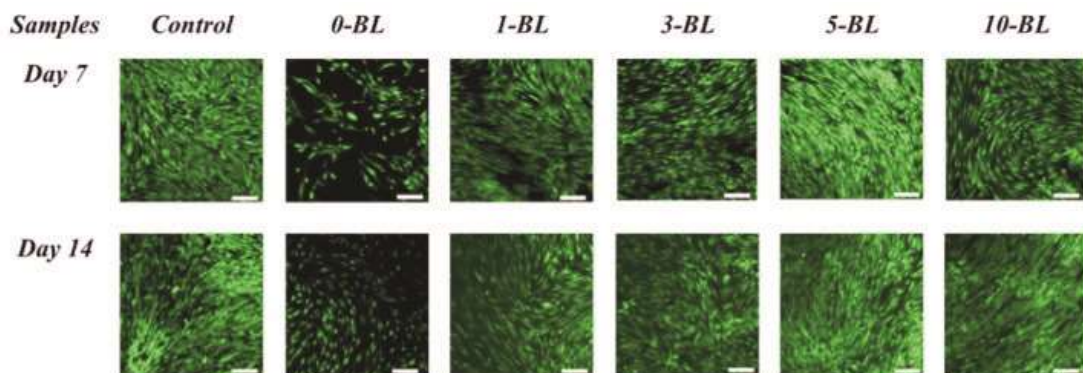


Figure 6

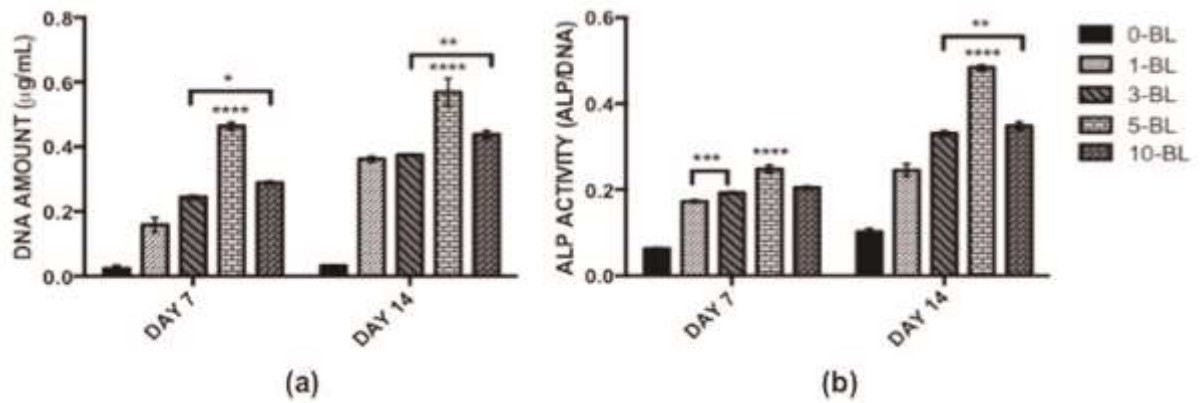


Table 1

<i>Samples</i>	C_{1s}	O_{1s}	N_{1s}	Ca_{2p}	P_{2p}	Si_{2p}
0-BL	77.74 ± 3.16	22.26 ± 3.16	-	-	-	-
0-BL*	76.42 ± 0.32	22.62 ± 0.34	1.96 ± 0.14	-	-	-
1-BL	73.83 ± 1.74	22.48 ± 1.54	2.07 ± 0.07	0.91 ± 0.03	0.47 ± 0.02	0.24 ± 0.18
3-BL	74.22 ± 1.12	19.19 ± 1.26	4.46 ± 0.51	1.21 ± 0.05	0.60 ± 0.02	0.32 ± 0.06
5-BL	74.09 ± 0.89	18.95 ± 0.66	4.92 ± 0.02	1.47 ± 0.05	1.12 ± 0.44	0.45 ± 0.26
10-BL	73.97 ± 0.97	18.86 ± 0.44	3.70 ± 0.34	1.39 ± 0.05	1.08 ± 0.05	0.42 ± 0.08

Table 2

<i>Surface roughness/ Samples</i>	<i>Whole area (nm)</i>	<i>Localized areas (nm)</i>
0-BL	52.83 ± 0.71	50.11 ± 0.91
1-BL	98.97 ± 0.97	96.48 ± 1.47
3-BL	177.33 ± 1.53	175.18 ± 2.71
5-BL	208.13 ± 0.80	214.98 ± 3.36
10-BL	186.37 ± 0.86	184.40 ± 2.10

Figure Captions

Fig. 1: Schematic of the natural bone extracellular matrix in the human body, consisting of collagen fibers, multi-substituted hydroxyapatite nanocrystals, non-collagenous polysaccharide, growth factors and protein.

Fig. 2: Schematic diagrams of (a) the mechanisms involved in aminolysis on PLA films and (b) the polyelectrolyte multilayers deposition technique. *Note: Hya=Hyaluronic acid, Coll I=Collagen type I, SiCHA=silicon-carbonated hydroxyapatite nanopowders, EDC=1-ethyl-3-(3-dimethylaminopropyl) carboiimide hydrochloride and NHS=N-hydroxysulfosuccinimide sodium salt.

Fig. 3: XPS survey spectra for different PLA surfaces and fitting analysis of the C1s, O1s, N1s and Ca2p spectra to quantify the different functional groups presents at the surface. Control PLA films, (a) before (0-BL) and (b) after (0-BL*) aminolysis, and coated PLA films (c) 1-BL, (d) 3-BL, (e) 5-BL and (f) 10-BL. The peak intensity of the materials detected on the surface is expressed in relation to the binding energy.

Fig. 4: (a) Alizarin Red (AR) and Sirius Red (SR) staining, and (b) Quantification on the amount of calcium and collagen deposited on different surfaces of PLA films. All coated PLA films showed positive stains for both AR and SR and the amount of stained material appeared to increase with the increasing number of layer, up to 5-BL. Quantitative data shown optimum amount of calcium and collagen were shown by 5-BL coated films ($n=3$). Scale bar=50 μm .

Fig. 5: Live/Dead assay of hMSCs cultured on control PLA films (0-BL) and coated PLA films deposited with 1-, 3-, 5-, and 10-BL. The green and red indicate live and dead cells, respectively. Cells seeded on the control PLA films were associated with a slower proliferation rate as fewer cells found on the surface compared to the coated PLA films. No dead cells were found on any PLA films. Scale bar=200 μm .

Fig. 6: (a) DNA content and (b) ALP activity of hMSCs after 7 and 14 days cultured on control PLA (0-BL) and PLA films deposited with different number of coating

layers of 1-, 3-, 5- and 10-BL, respectively. 5-BL shows the highest DNA concentration and ALP activity after 7 and 14 days in culture compared to other films ($p \leq 0.0001$). [$n=3$, $*p<0.05$, $**p<0.01$, $***p<0.001$ and $****p<0.0001$].

Table Titles

Table 1: Atomic percentage (at%) of the control PLA (0-BL) and coated PLA with 1-, 3-, 5- and 10-BL, respectively. [$n=3$, means \pm SD].

Table 2: Surface roughness of PLA films measured on the control PLA (0-BL) and coated PLA with 1-, 3-, 5- and 10-BL, respectively. [$n=3$, means \pm SD].